Electronic structure and optical transition of semiconductor nanocrystallites

1997 J. Phys.: Condens. Matter 9 9853

(http://iopscience.iop.org/0953-8984/9/45/013)

J. Phys.: Condens. Matter **9** (1997) 9853–9862. Printed in the UK PII: S0953-8984(97)83795-2

Electronic structure and optical transition of semiconductor nanocrystallites

Jian-Bai Xia and K W Cheah†

Department of Physics, Hong Kong Baptist University, Kowloon Tong, Hong Kong

Received 29 April 1997, in final form 23 June 1997

Abstract. The electronic states and optical transition properties of three semiconductor nanocrystallites, Si, GaAs, and ZnSe, are studied using the empirical pseudopotential homojunction model. The energy levels, wave functions, optical transition matrix elements, and lifetimes are obtained for quadratic prisms with widths from 11 to 27 Å. It is found that the three kinds of prism have different quantum confinement properties. For Si prisms, the energy gaps vary with the equivalent diameter d as $d^{-1.37}$, in agreement with previous theoretical calculations. For the same d the energy gaps are slightly different for different shapes: large for the prism with large aspect ratio; small for the prism with small aspect ratio. The exponent of d depends on the boundary barrier height, i.e. the extent of penetration of the wave function into the vacuum. The wave function of the LUMO states consists mainly of bulk X states. The optical transition matrix elements are much smaller than those of direct transition, and increase with decreasing width. The corresponding lifetimes decrease from the millisecond range to the microsecond range, and the change is abrupt depending on the symmetry and composition of the wave function of the LUMO and HOMO states. For GaAs prisms, the energy gap is also pseudo-direct, but the optical transition matrix elements are larger than those of Si prisms by two orders of magnitude for the same width. For ZnSe prisms, the energy gap is always direct, and the optical transition matrix elements are comparable with those of direct energy gap bulk semiconductors. In some cases the symmetry of the HOMO state changes, resulting in an abrupt decrease of the transition matrix element. The calculated lifetimes of the Si prism and the positions of PL peaks are in agreement with experimental results for porous Si.

1. Introduction

Recent observations of visible photoluminescence (PL) in porous Si [1] and Si nanocrystallites [2–7] suggest that Si nanoclusters may become promising material for optical applications. The visible photoluminescence has been observed in Si nanocrystallites embedded in an Si oxide matrix, [2, 3] Si nanocrystal colloid, [4] and Si nanoclusters passivated with oxygen [5–7]. However, the measured emission intensity, lifetime, and temperature dependence show a strong sensitivity to surface processing, such as chemical treatment and oxidation. There has been much theoretical research on the Si nanocluster to study the quantum confinement effect, including tight-binding calculations [8, 9], density-functional pseudopotential calculations [10, 11], empirical pseudopotential calculation [12], and the two-particle calculation [13] including the electron–hole Coulomb interaction nonpertubatively. On the other hand the direct gap semiconductor nanocrystals, such as CdSe, have been extensively studied [14–16]. The transition from the lowest unoccupied state (LUMO) to highest occupied state (HOMO) is electric dipole allowed for all sizes.

† Fax: 852-23046558. E-mail address: kwcheah@hkbc.edu.hk

0953-8984/97/459853+10$19.50

In this paper we study how the electronic structure of either indirect or direct energy gap semiconductors changes from bulk to nanocrystallites. We use the empirical pseudopotential homojunction model [17, 18] to calculate the electronic states and their corresponding optical transition probabilities (i.e. lifetimes) for semiconductor nanoclusters, namely Si, GaAs, and ZnSe. Because in our calculation the wave functions of the nanocrystal can be composed of energy band states of the bulk semiconductor, the LUMO states and HOMO states can be clearly correlated with the bulk band states at various special points of the Brillouin zone. Section 2 gives the theoretical method. sections 3 and 4 give results for the Si and GaAs, ZnSe nanocrystallites, respectively. Section 5 contains the summary.

2. Empirical pseudopotential homojunction model [17, 18]

We use the super-cell model to study quadratic prisms, which are arranged periodically in three-dimensional space. The system has translational symmetries in the [110], [$\bar{1}$10], and [001] directions with periods $(l\sqrt{2}/2)a$, $(l\sqrt{2}/2)a$, and ma, where l and m are integers which determine the size of the unit cell and a is the lattice constant. Because of the periodicity of the system, the wave function of the prism can be written in terms of its bulk states with wave vectors $\boldsymbol{g}$, where $\boldsymbol{g}$ are reciprocal-lattice vectors of the model system enclosed within the first Brillouin zone of bulk material. Here we use the double unit cell with the basic vectors

$$\boldsymbol{a}_1 = \frac{a}{2}(1, 1, 0) \qquad \boldsymbol{a}_2 = \frac{a}{2}(-1, 1, 0) \qquad \boldsymbol{a}_3 = a(0, 0, 1) \tag{1}$$

instead of the usual unit cell of the diamond structure in order to satisfy the periodicity. The components of $\boldsymbol{g}$ along the [110], [$\bar{1}$10] and [001] directions are given by

$$g_1 = \frac{2\pi}{l(\sqrt{2}/2)a} l_1 \tag{2}$$

$$g_2 = \frac{2\pi}{l(\sqrt{2}/2)a} l_1 \tag{3}$$

$$l_1 = -[(l-1)/2], \ldots, 0, \ldots, [l/2] \tag{4}$$

$$g_3 = \frac{2\pi}{ma} m_1 \tag{5}$$

$$m_1 = -[(m-1)/2], \ldots, 0, \ldots, [m/2] \tag{6}$$

where we have used the symbol $[x]$ to denote an integer closest to but not larger than x. Using these bulk states as basis functions for the expansion of the wave functions of the prism, we have

(7)

where $\psi_{n,g}$ represents the bulk Bloch states associated with the nth band and wave vector $\boldsymbol{g}$.

We assume that the space between prisms is unfilled and can be considered as vacuum region. Then, the perturbation potential in the vacuum region between prisms $\Delta V(\boldsymbol{r}) = V_0$, while in the prism region $\Delta V(\boldsymbol{r}) = 0$, where V_0 is large relative to the energy range considered. It is positive for the conduction-band states and negative for the valence-band states. Namely, the vacuum regions are replaced by the same bulk material with the conduction bands rigidly shifted upward by a constant and the valence bands shifted downward by another constant. The problem now resembles that of a homojunction. The mixing of conduction-band state and valence-band states is neglected by solving the problem

separately for conduction and valence bands. That means that first we project all the plane waves on to the bulk conduction-band state subspace and the bulk valence-band subspace, then calculate the electron and hole states of the prism in these two subspaces, respectively. This is a reasonable approximation because the energy gap between the electron states and hole states increases with the quantum confinement strengthening, and the mixing of conduction-band states and valence-band states can be neglected.

Using degenerate perturbation theory, we obtain a secular equation for the prism,

$$|E_{n,\boldsymbol{g}}\delta_{nn'}\delta_{\boldsymbol{g}\boldsymbol{g}'} + \langle n, \boldsymbol{g}|\Delta V|n', \boldsymbol{g}'\rangle - E| = 0 \tag{8}$$

where $E_{n,\boldsymbol{g}}$ is the energy eigenvalues of the bulk. In the coordinate system with x, y and z axes along the [110], [$\bar{1}$10], and [001] directions, respectively, the matrix elements of the perturbation potential can be obtained for the plane wave basic function.

The form factors of the empirical pseudopotential $V_S(3)$, $V_S(8)$, $V_S(11)$, and $V_A(3)$, $V_A(4)$, $V_A(11)$ are not enough for the double-unit-cell energy band calculation, so we fit the atomic form factors by an analytical formula. For Si we use the analytical formula given by Wang and Zunger [12], and for GaAs and ZnSe, we use the following analytical formulae (in units of Ryd):

$$\begin{aligned} V(q) &= \frac{a_1 + a_2 q^{a_4}}{1 + \exp(a_5(q - a_6))} && \text{for Ga} \\ V(q) &= \frac{a_1 + a_2 \exp(a_3 q^{a_4})}{1 + \exp(a_5(q - a_6))} && \text{for As, Se} \\ V(q) &= \frac{a_1 + a_2 \exp(a_3(q - q_0)^{a_4})}{1 + \exp(a_5(q - a_6))} && \text{for Zn} \end{aligned} \tag{9}$$

where the coefficients a_1–a_6 and the lattice constant a are given in table 1.

Table 1. Coefficients a_1–a_6 of atomic form factors for Ga, As, Zn, and Se and lattice constants of GaAs and ZnSe.

	a_1	a_2	a_3	a_4	a_5	a_6	a (Å)
Ga	−0.4456	0.2577		1.1794	18.77	2.0243	5.6419
As	0.2364	−0.884	−0.4801	1.946	9.903	1.9887	
Zn	−0.1289	0.23	−1.23	2	21.31	2.05	5.65
Se	0.15	−1.01	−0.567	2	15.45	2.1	

The optical transition matrix elements and corresponding lifetime are given by

$$Q^i_{nn'} = \frac{1}{m_0}|\langle n|p_i|n'\rangle|^2 \qquad i = x, y, z \tag{10}$$

and

$$\frac{1}{\tau} = \frac{4\alpha\omega n}{3m_0c^2} Q_{nn'} \tag{11}$$

where α is the fine-structure constant, ω is the photon angular frequency and n is the refractive index.

3. Results for an Si quadratic prism

In all calculations in this paper we take $l = 7$, $m = 7$, and four lowest conduction-band states or four highest valence-band states of the bulk as basis functions, hence we have only

1372 basis functions in the wave-function expansion. The V_0 values are taken as 3.2 and -2.4 eV for the conduction-band and valence-band states, respectively.

The eigenenergies of the four LUMO states and the four HOMO states for $l_1 = 5, 4, 3$, and $m_1 = 5, 4, 3, 2$ structures are obtained. We found that in some cases the energies of the four LUMO states are close, for example, $l_1 = 5$, $m_1 = 5$; $l_1 = 4$, $m_1 = 5, 4$; and $l_1 = 3$, $m_1 = 5, 4, 3$, i.e. the case of normal aspect ratio, but for the cases of smaller aspect ratio only the energies of the two LUMO states are close. From the wave functions it is clear that for the former case the wave functions are composed of four bulk conduction-band states at X points in the XY-plane of the Brillouin zone, while for the latter case the wave functions are composed of two conduction-band states at X points on the Z-axis of the Brillouin zone. This can also be verified by the effective-mass theory. For the same confinement condition we calculated the energy of the X state electron by the effective-mass equation. For the X states in the XY-plane, the equation is given by

$$-\frac{\hbar^2}{2}\left[\frac{1}{2}\left(\frac{1}{m_1}+\frac{1}{m_2}\right)\left(\frac{\partial^2}{\partial x^2}+\frac{\partial^2}{\partial y^2}\right)+\left(\frac{1}{m_1}-\frac{1}{m_2}\right)\frac{\partial^2}{\partial x\,\partial y}+\frac{1}{m_2}\frac{\partial^2}{\partial z^2}\right]f(\boldsymbol{r})+V(\boldsymbol{r})f(\boldsymbol{r}) = Ef(\boldsymbol{r}). \tag{12}$$

That for the X states on the Z-axis is given by

$$-\frac{\hbar^2}{2}\left[\frac{1}{m_2}\left(\frac{\partial^2}{\partial x^2}+\frac{\partial^2}{\partial y^2}\right)+\frac{1}{m_1}\frac{\partial^2}{\partial z^2}\right]f(\boldsymbol{r})+V(\boldsymbol{r}) = Ef(\boldsymbol{r}) \tag{13}$$

where m_1 and m_2 are the effective mass of the electron state near the X point parallel and perpendicular to the main axis of the energy ellipsoid sphere, respectively. Solving equations (12) and (13) we obtain the same results as the pseudopotential calculation, i.e., for the case of normal aspect ratio, the energy of the electron at the X state in the XY-plane is lower than the energy of the electron on the Z-axis, and *vice versa* in the case of smaller aspect ratio. Because $m_1 \gg m_2$, for the case of smaller aspect ratio the electron at the X point on the Z-axis is confined in the narrow Z-direction with the large effective mass m_1, whereas in the wide X-and Y-directions with very small effective mass m_2, its energy will be relatively low compared to that in the XY-plane. The four or two lowest X states and the Γ state couple to each other due to the quantum confinement effect, forming the LUMO states of the prism. In fact the ground LUMO state (C1) is always singlefold, which is totally symmetric with respect to the X-, Y-, or Z-plane. The excited states are asymmetric with respect to the X-, Y-, or Z-plane. The HOMO states are mainly composed of bulk valence band states from the Γ point and nearby states. We also found that the two HOMO states are nearly degenerate, and are composed of the highest four states of the valence band for the crystal with the double unit cell.

The energy gap as a function of the equivalent diameter $d = [6V/\pi]^{1/3}$ of the prism is shown in figure 1, where d is the diameter of a sphere that has the same volume as the prism. From figure 1 we see that the energies increase with decreasing width, but the variation is not at a unified curve. There are three groups of data, each for a fixed transverse width $l_1 b$ ($l_1 = 3, 4, 5$, corresponding to large-, medium- and small-aspect-ratio prisms, respectively). Four points in each group correspond to longitudinal lengths $m_1 a$, $m_1 = 2, 3, 4, 5$. From figure 1 we see that the prism with large aspect ratio has a larger energy gap, and the prism with small aspect ratio has a smaller energy gap, relatively. This result is consistent with the results of Wang and Zunger [12]. The curves in figure 1 represent the variation of energy gap with the equivalent diameter d as $d^{-1.37}$ and $d^{-1.39}$, given by previous theoretical calculations ([12] and [9] respectively). In fact the exponent -1.37 (or -1.39) represents the degree of penetration of the wave function into the vacuum

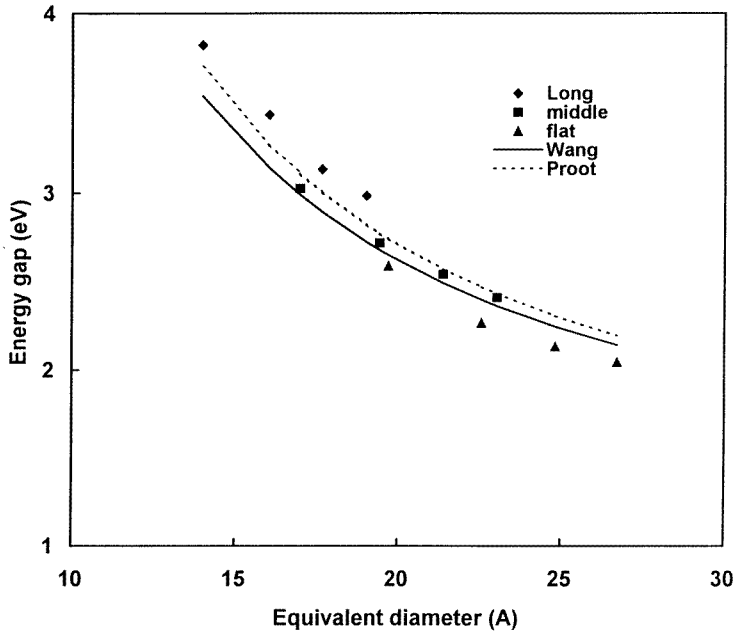

Figure 1. Calculated LUMO–HOMO energy gaps as a function of equivalent diameter for Si quadratic prisms, compared with previous theoretical calculations. 'Long', 'Middle', and 'Flat' refer to prisms of widths 3, 4, and 5 ($a/\sqrt{2}$), respectively. The solid and dashed lines are theoretical results of [12] and [9], respectively.

at the surface of the prism. If we take the potential barrier height V_0 as infinite we will obtain the exponent of the effective-mass theory, -2.00, and if we take V_0 larger than that used in the present calculation we will obtain an exponent between -1.37 and -2.00. The tight-binding calculation [9] and the empirical pseudopotential calculation [12] all assumed that the boundary of the silicon clusters is totally passivated by hydrogen atoms, and obtained the nearly same exponent: -1.39 and -1.37, respectively. This means that the authors have taken suitable interaction parameter between the silicon and hydrogen atoms, though in different models. When oxygen or other atoms passivate the boundary of the Si clusters, the degree of penetration of the wave function into vacuum will be different, and then we will obtain a different exponent of the variation of the energy gap.

Using (10) we calculated the optical transition matrix elements for C1 and C2 states to V1 and V2 states. It was found that the optical transition matrix elements are small compared to the direct transition as in bulk GaAs (a few electron volts), which means the energy gap is pseudo-direct, as shown by the wave function composition. When the width l_1 and length m_1 of the prism decrease the optical transition matrix elements increase due to the mixing of the bulk Δ states and near-Γ states. When the composition of the ground LUMO state changes from mainly four bulk X states in the XY-plane of the Brillouin zone to two bulk X states on the Z-axis for the small-aspect-ratio structures, there is an abrupt increase of the optical transition matrix elements for the ground LUMO state (C1) to the ground HOMO state (V1). The matrix elements increase by about three orders of magnitude (typically from 10^{-7} to 10^{-4} eV) for the cases of $l_1 = 5$ and 4, and increase by one order of magnitude from 10^{-5} to 10^{-4} eV for the case of $l_1 = 3$, as m_1 decreases from five to two. Using (11) we calculated the lifetimes of the transition for the C1 state to the V1 state,

which are shown in figure 2. From figure 2 we see clearly the abrupt change of the lifetime, from the millisecond range to the microsecond range or less. These results can explain why all the theoretical calculations [9, 11, 12] always obtained divergence for transition matrix elements (or lifetimes), but relatively unified energy gaps. The transition matrix element depends sensitively on the shape of the cluster, i.e. the composition of the wave function of the ground LUMO state.

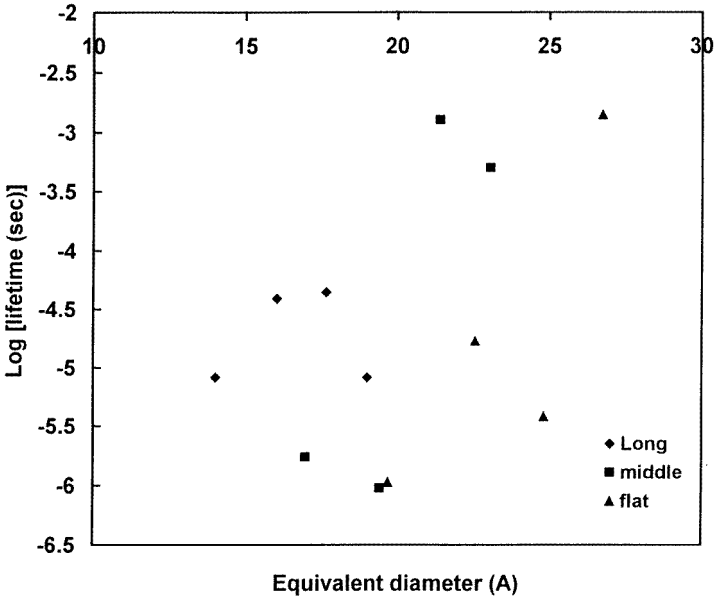

Figure 2. Radiative lifetimes as a function of equivalent diameter for Si quadratic prisms.

We compare our theoretical results with the room-temperature time-resolved PL experiment for porous Si [19]. The main emission peaks and lifetimes observed by Calcott *et al* are schematically shown in figure 3. If we consider the $l_1 = 5$ (19.2 Å), $m_1 = 5$ (27.2 Å) results, we see that the lowest transitions are C1–V1(V2) and C2–V1(V2) (because V1 and V2 are degenerate); the optical transition energies are 2.046 and 2.062 eV, respectively, with an energy difference of 16 meV. The corresponding optical transition matrix elements $Q_{nn'}$ (10) are 7.37×10^{-7} and 5.04×10^{-5} eV, respectively. Inserting the $Q_{nn'}$ into (11) ($n = 2.6$), we obtain lifetimes of 1.4 ms and 20 μs respectively, which are in agreement with the experiment. This result verifies that there exist optical transitions between quantum confinement states in porous silicon, though the luminescence strength is not large enough to explain the strong luminescence. For the normal aspect ratio structures though, the transition matrix elements are small for the C1–V1 transitions, but increase by three to four orders of magnitude for the C2–V1 transitions, just as in the above case. The energy difference between the C1 and C2 states ranges from a few millielectron volts to 20 meV, therefore the room-temperature luminescence of the porous or nanocrystallite Si may be more efficient than the low-temperature luminescence.

It was found that the experimental PL energy is generally smaller than the theoretical energy gap (or exciton energy) for the Si nanocrystals of the same size [6, 7]. Hill and Whaley [13] obtained smaller exciton energies in agreement with the measured PL energies. They attributed the agreement to the accuracy of their tight-binding description with the

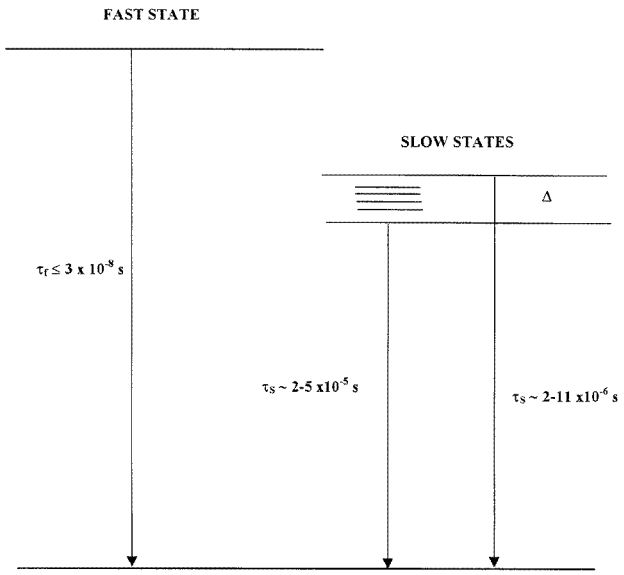

Figure 3. A schematic depiction of the main emission peaks and lifetimes observed by Calcott *et al* [19] for porous Si.

expanded basis, rather than the non-perturbative Coulomb treatment. We propose another reason. The exciton energy for a sphere is usually calculated by [12, 20]

$$E_x = E_{gap} - \frac{3.572}{\epsilon d} - 0.248E_{Ry} \tag{14}$$

where the second term is the Coulomb term, and the third term is a correlation energy correction. ϵ is the dielectric constant, and $E_{Ry} = \mu e^4/\epsilon^2\hbar^2$; μ is the reduced mass of an electron–hole pair. One generally used the bulk Si value $\epsilon = 11.91$ and $E_{Ry} = 8.18$ meV, and the resulting E_x correction is much smaller than the energy gap except for very small diameters [12].

Actually since the Si nanocrystals are surrounded by air, the image charges will have a large effect on the effective Coulomb potential in spheres. We calculated the image charge effect in isolated quantum wires [21], and found that the effective potential approaches the Coulomb potential in vacuum at large z-distance. The exciton binding energy is much larger than that in the bulk. For example: for a isolated Si wire of radius 15 Å, the effective radius is $0.2a_B(\epsilon\hbar^2/\mu e^2)$. From figure 2 of [21] we obtain the exciton binding energy $E_x = 60E_{Ry} = 0.49$ eV. We expect that the exciton binding energy will be larger for the isolated Si sphere with the same radius. This work is in progress.

4. Results for GaAs and ZnSe nanocrystallites

Our model can be applied equally to other semiconductor nanocrystallites, because the model does not impose any restriction condition on the boundary, only a constant potential barrier. For the GaAs and ZnSe nanocrystallites we take 'harder' boundary barriers: $V_0 = 8$ and -6 eV for the LUMO and HOMO states, respectively. The energy gaps as functions of the equivalent diameter are shown in figure 4. From figure 4 we see that the energy gaps vary with the equivalent diameter d as $d^{-1.477}$ and $d^{-1.655}$ for the GaAs and ZnSe prisms,

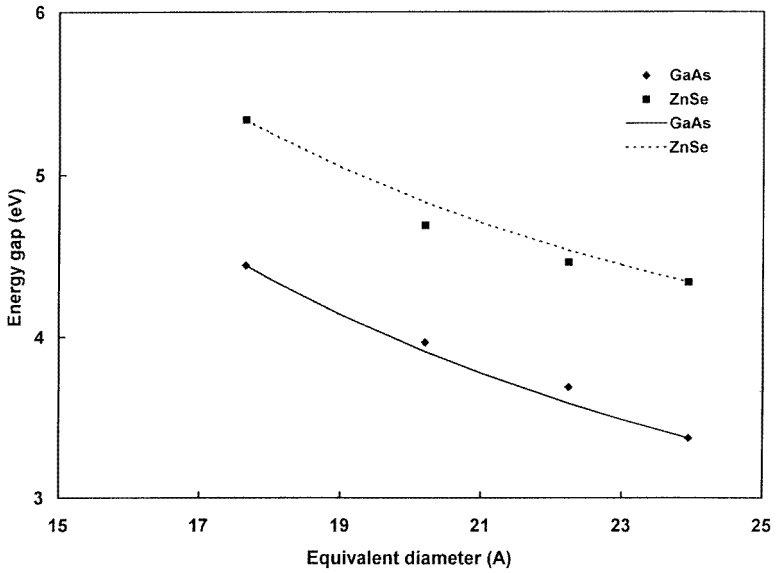

Figure 4. Calculated LUMO–HOMO energy gaps as functions of the equivalent diameter for GaAs and ZnSe prisms of width 4 ($a/\sqrt{2}$). The solid and dashed lines are curves fitted as $d^{-1.477}$ (GaAs) and $d^{-1.655}$ (ZnSe), respectively.

respectively. The exponent factors depend on the potential barrier height used. The wave functions of the GaAs prisms are mainly composed of bulk X states: four X states in the XY-plane of the Brillouin zone for the $m_1 = 5, 4$ cases, and two X states on the Z-axis for the $m_1 = 3, 2$ cases, just as in the case of silicon. This means that the GaAs prisms of small size become indirect gap, which has been predicted for the cases of dot [22] and wire [18]. For the bulk energy band of GaAs the Γ and L states are all lower than the X states, due to the smaller effective masses of the Γ and X energy valleys; under the same confinement condition the quantum states of these two valleys become higher than that of the X valley, which can be checked by effective-mass equations similar to (10) and (11). Therefore, there are four or two LUMO states with close energies, composed of bulk X states. On the other hand, for ZnSe prisms the wave functions of the LUMO states are mainly composed of bulk Γ and near states, hence the LUMO state is singlefold. Unlike the case of silicon, the two HOMO states are not twofold degenerate for the GaAs and ZnSe cases (except for the GaAs of $l_1 = 4$ and $m_1 = 2$), while the second and third HOMO states or the third and fourth HOMO states are twofold degenerate.

Though the GaAs prism is indirect energy gap, the optical transition matrix elements are larger than those of the Si prisms by about two orders of magnitude for the same width, and increase with decreasing width. In the case of $m_1 = 3$ the transition matrix element of the C1–V1 transition becomes unexpectedly small (10^{-6} eV), which is caused by the change of symmetry in the HOMO state. This point will be discussed below. The ZnSe prisms are always direct energy gap with large optical transition matrix elements ($\sim$eV). Because the bulk X states are far higher than the bulk Γ_1 state by 1.7 eV, and furthermore the effective mass of the ZnSe Γ_1 state is relatively large ($0.15m_0$), the bulk Γ_1 state is always lower than the bulk X states as the width of prism decreases. For the cases of $m_1 = 3$ and 2 the optical transition matrix elements of the C1–V2 transition are large, while

those of the C1–V1 transition are very small. It is also caused by the change of symmetry of the V1 state. The wave function of these V1 states consist of no components of bulk Γ state and states on the Z-axis of the Brillouin zone, which are similar to the T_1 state predicted by the tight-binding cluster model [23]. Experimentally it is found that a II–VI compound semiconductor cluster of 20–200 Å shows good luminescence character [14–16]; our results prove theoretically that the optical transition is direct in these thin quantum wires or dots, and gives a good prospect for them in practical applications. Theoretically one of the present authors (J B Xia) has proposed a spherical tensor model [24, 25] based on the effective-mass theory to deal with the HOMO states of the semiconductor nanosphere, but from the present calculation it seems that for very thin nanocrystallites the HOMO states will have different symmetry due to mixing of the central and edge states in the Brillouin zone, which is beyond the applicable range of the effective-mass theory.

5. Summary

In this paper we studied the electronic states and optical transition properties of three semiconductor nanocrystallites, Si, GaAs, and ZnSe, using the empirical pseudopotential homojunction model. The energy levels, wave functions, optical transition matrix elements, and lifetimes are obtained for quadratic prisms with width from 14 to 27 Å. It is found that the three kinds of prism have different quantum confinement properties. For Si prisms, the energy gaps vary with the equivalent diameter d as $d^{-1.37}$, in agreement with previous theoretical calculations. For the same d the energy gaps are slightly different for different shapes: large for the prism with large aspect ratio; small for the prism with small aspect ratio. The exponent of d depends on the boundary barrier height, i.e. the penetration extent of the wave function into the vacuum. The wave function of the LUMO states consists of mainly bulk X states: four X states in the XY-plane of the Brillouin zone in the case of normal aspect ratio; two X states on the Z-axis in the case of small aspect ratio. The optical transition matrix elements are much smaller than that of direct transition, and increase with decreasing width. The corresponding lifetimes decrease from the millisecond range to the microsecond range, and the change is abrupt depending on the symmetry and composition of the wave function of the LUMO and HOMO states. For GaAs prisms, the energy gap is also pseudo-direct, but the optical transition matrix elements are larger than those of Si prisms by two orders of magnitude for the same width. For the ZnSe prisms, the energy gap is always direct, and the optical transition matrix elements are comparable with those of direct energy gap bulk semiconductors. In some cases the symmetry of the HOMO state changes, resulting in an abrupt decrease of the transition matrix element. The calculated lifetimes of the Si prism, and the positions of PL peaks are in agreement with experimental results for porous Si [19]. The potential barrier height V_0 values in our model do influence the energy gap and the exponent of their variations. The V_0 values for Si taken in this paper are fitted to the energy gap results of the tight-binding and empirical pseudopotential calculations [11, 12]. The V_0 has physical meaning as the band offset between the quantum dot and the surrounding material. For example, if we take V_0 as the band offset between Si and SiO_2, then we can study Si quantum dots embedded in SiO_2. In the case of an Si quantum dot in vacuum with H_2 saturated dangling bonds, there are no experimentally determined V_0 values for the conduction band and valence band, so we can only fit them by comparing with other theoretical calculations which have taken into account the interaction between Si and H atoms. For GaAs and ZnSe, we take larger V_0 values to simulate the case of quantum dots in vacuum. On the other hand, it was found that the wavefunctions and the optical transition elements are less affected by the V_0 values.

Thus our model is suitable for studying the quantum confinement effect caused by the shape and volume of the material, and the V_0 values can represent different interface cases. This theoretical model has some advantages compared to the direct pseudopotential calculation. Our calculation is actually a variation in calculation for the LUMO states and HOMO states. Therefore if we take relatively complete basic functions, the LUMO states and HOMO states can be calculated accurately. While in the direct pseudopotential or tight-binding cluster calculations all states below the energy gap should be calculated, the needed states around the energy gap are higher than all the other states which contribute very little to the optical transition. The wave functions calculated by our model consist obviously of components of bulk states in the Brouillon zone, so it is convenient for analysis of the transition property. Our model does not put any restriction condition on the boundary, hence it can be applied to any semiconductor nanocrystallites, and takes into account the pure quantum confinement effect.

Acknowledgment

This work was supported by a Croucher Foundation Research Grant.

References

[1] Canham L T 1990 *Appl. Phys. Lett.* **57** 1046
[2] Takagi H, Ogawa H, Yamazaki Y, Ishizaki A and Nakagiri T 1990 *Appl. Phys. Lett.* **56** 2379
[3] Zhang Q, Bayliss S C and Hull D A 1995 *Appl. Phys. Lett.* **66** 1977
[4] Littau K A, Szajawski P J, Muller A J, Kortan A R and Brus L E 1993 *J. Phys. Chem.* **97** 1224
[5] Brus L E, Szajawski P F, Wilson W L, Harris T D, Schuppler S and Citrin P H 1995 *J. Am. Chem. Soc.* **117** 2915
[6] Schuppler S *et al* 1995 *Phys. Rev.* B **52** 4910
[7] Dinh L N, Chase L L, Balboch M, Siekhaus W J and Wooten F 1996 *Phys. Rev.* B **54** 5029
[8] Ren S Y and Dow J D 1992 *Phys. Rev.* B **45** 6492
[9] Proot J P, Delerue C and Allan G 1992 *Appl. Phys. Lett.* **61** 1948
[10] Hirao M, Udo T and Murayama Y 1993 *Mater. Res. Soc. Symp. Proc.* **283** 425
[11] Delley B and Steigmeier E F 1993 *Phys. Rev.* B **47** 1397
[12] Wang L W and Zunger A 1994 *J. Phys. Chem.* **98** 2158
[13] Hill N A and Whaley B 1995 *Phys. Rev. Lett.* **75** 1130
[14] Steigerwald M L, Alivisatos A P, Gibson J M, Harris T D, Kortan K R, Muller A J, Thayer A M, Duncan T M, Douglass D C and Brus L E 1988 *J. Am. Chem. Soc.* **110** 3046
[15] Kortan A R, Hull R, Opila R L, Bawendi M G, Steigerwald M L, Carroll P J and Brus L E 1990 *J. Am. Chem. Soc.* **112** 1327
[16] Murray C B, Norris D J and Bawendi M G 1993 *J. Am. Chem. Soc.* **115** 8706
[17] Xia J B and Chang Y C 1993 *Phys. Rev.* B **48** 5179
[18] Xia J B and Cheah K W *Phys. Rev.* B submitted
[19] Calcott P D J, Nash K J, Canham L T, Kane M J and Brumhead D 1993 *J. Phys. C: Solid State Phys.* **5** L91
[20] Brus L E 1986 *J. Phys. Chem.* **90** 2555
[21] Xia J B and Cheah K W 1997 *Phys. Rev.* B **55** 1596
[22] Wang L W and Zunger A 1996 *Phys. Rev.* B **54** 11 417
[23] Ren S Y 1997 *Phys. Rev.* B **55**
[24] Xia J B 1989 *Phys. Rev.* B **40** 8500
[25] Xia J B 1996 *J. Lumin.* **70** 120